Benchmarking 2D against 3D FDTD codes in the assessment of reflectometry performance in fusion devices

Filipe da Silva, Stéphane Heuraux, Emanuel Ricardo, Antonio Silva, Tiago Ribeiro

Benchmarking 2D against 3D FDTD codes in the assessment of reflectometry performance in fusion devices

F. da Silva,[a] S. Heuraux,[b] E. Ricardo,[a] A. Silva[a] and T. Ribeiro[c]

[a] *Instituto de Plasmas e Fusão Nuclear, Instituto Superior Técnico, Universidade de Lisboa, 1049-001 Lisboa, Portugal*

[b] *Institut Jean Lamour UMR 7198 CNRS-Université de Lorraine, ARTEM BP 50840, F-54011 Nancy, France*

[c] *Max-Planck-Institut für Plasmaphysik, Garching D-85748, Germany*

E-mail: tanatos@ipfn.tecnico.ulisboa.pt

Abstract: Reflectometry is foreseen in the coming generation of tokamaks such as DTT, ITER and DEMO, creating a need to predict the behavior and capabilities of these new reflectometry systems through the used of synthetic diagnostics. The FDTD time-dependent codes use to implement synthetic diagnostics are computational demanding, the reason why 2 dimensional codes (as REFMUL or REFMULF) are used. REFMUL3, a newly developed performing parallel code gives access to 3D simulations, although at a much higher cost than the 2D ones. With this work we begin a benchmark effort to assess the main differences and compromises done when using 2D versus 3D.

Keywords: Simulation methods and programs; Plasma diagnostics - interferometry, spectroscopy and imaging

Contents

1 Introduction

Reflectometry, an important technique to diagnose fusion plasmas, is foreseen in the coming generation of machines such as DTT, ITER and DEMO. There is a real need to predict the behaviour and capabilities of these new reflectometry systems. Synthetic diagnostics using FDTD time-dependent codes permit a comprehensive view of reflectometry, including aspects such as propagation in the plasma, the system location within the vacuum vessel, its access to the plasma or the signal processing techniques. To obtain a relevant description of the phase, the spatial discretisation used by FDTD is a small fraction of the wavelength, a fact that together with the physical size of the regions of interest considered leads to very large simulations domains (number of grid points). Time discretisation is also a small fraction of the probing wave period due to the need to comply with the CFL condition. These two facts make reflectometry simulation computational demanding, the main reason why two dimensional codes (2D), as REFMUL or REFMULF, are used. REFMUL3, a newly developed performing parallel code gives access to three dimensional (3D) simulations, although much more costly than 2D ones. We are benchmarking the two types of codes to assess the main differences, such as the amplitude of reflected signal, and compromises done when using 2D versus 3D. This is essential to improve data processing for the initialization problem and density profile reconstruction, taking into account multi-reflections and edge turbulence effects on the properties of probing beam or to extract the characteristics of the electron density fluctuations.

2 Finite-difference time-domain codes for reflectometry simulation

The main computational electromagnetics (CEM) technique used to simulate reflectometry is finite-difference time-domain (FDTD) by solving Maxwell curl equations in a vacuum and coupling the plasma physics through a source term due to the current density $\mathbf{J}$ [1]. The current density is handled through an auxiliary linear differential equation (LDE). This equation system is solved using the Yee schema for the curl equations [2], and a time integrator for the LDE. In this work we are using REFMUL, a 2D Ordinary mode (O-mode) and REFMUL3, a 3D code.

3 Simulation setup

As the start point for the 2D-3D benchmark this work intends to be, we propose a simple model consisting of a slab plasma with a linear evolution of the electronic density $n_e(R)$, with R being the distance along the Line of Sight (LoS) taken along the antenna axis and perpendicular to the iso-denstities. The 3D simulation box is $2000\times1500\times1500$ grid points while the 2D box is reduced to 2000×1500. For a $\lambda_{40\,\mathrm{GHz}}$ this corresponds to a box/plane of $75(\times56)$ cm. The x-y-z directions correspond in a tokamak to the radial, poloidal and toroidal directions. In 2D the plane of simulation is a poloidal section of the torus. In figure 1—left we show the 3D simulation setup with a piramidal horn and the LoS. The evolution of n_e along the LoS transversing the plasma slab is displayed at the right. The plasma edge is located radially at $R_0 = 250$ grid points (9.4 cm). The vacuum distance between the antenna mouth and R_0 is $d_v = 50$ grid points (1.12 cm). The density evolves with a gradient of $L = 1.32\times10^{16}\,\mathrm{m}^{-3}$/grid point ($L = 3.52\times10^{19}\,\mathrm{m}^{-4}$). The plasma is probed using frequency modulated continuous wave (FMCW) in the Ka band from 30 GHz to 40 GHz which covers a density range of $1.1\text{–}2\times10^{19}\,\mathrm{m}^{-3}$, shown by the shaded area in figure 1—right. The simulations run for 120,000 iteration steps. As an antenna we use a pyramidal horn having flare angles of $2\psi_h = 14°$ in the H-plane and $2\psi_e = 7°$ in the E-plane and a length of $p = 100$ grid points. The antenna is placed having the H-plane poloidally. For the 2D simulations a 2D version of the antenna consisting of a cut though the H-plane is used. The horn radiation diagram differs considerably from the H- to the E-planes [3] and in figure 2—left we can observe this differences in the electric field E_z snapshots of the H-plane and E-planes, taken at iteration $t_k = 100\times10^3$. The beam in the H-plane (x-y) is narrower. Also on the larger E-plane beam (x-z) the existence of an important side lobe is clear, together with a lower front-to-back ratio.

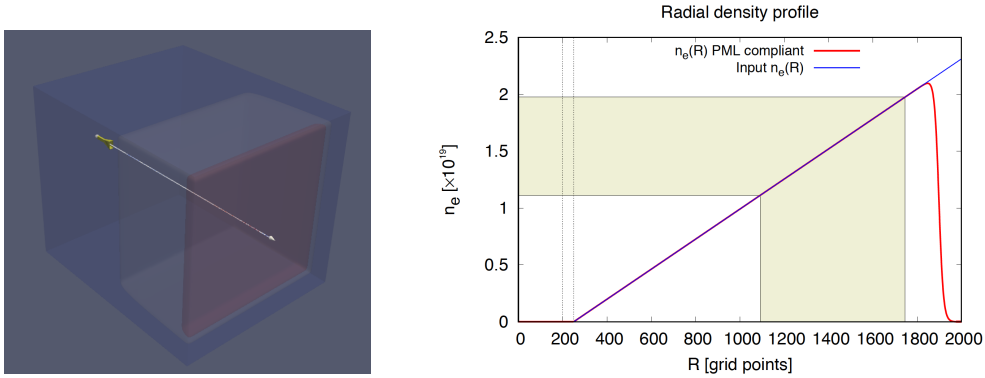

Figure 1. On the left, the 3D simulation setup showing the horn antenna and the 3D slab plasma. Along the axial direction, marked with the white arrow, the density $n_e(R)$ evolves linearly as shown on the right. The shadowed region indicates the density coverage of the Ka frequency band.

4 Simulations

Three antenna setups were employed: (i) a monostatic (MONO) setup for sending (Tx)/receiving (Rx); (ii) a bistatic configuration with the antennas toroidally distributed (BTOR); and (iii) a bistatic configuration with the antennas poloidally distributed. Note that the 2D version of (ii) cannot be

implemented since the 2D simulation plane is a poloidal one, through the H-plane of the antenna and in this configuration the antennas are toroidally separated along the 3rd dimension. This is nonetheless a common experimental setup and traditionally, in 2D simulations, the BTOR distribution is approximated by 2D MONO simulations, considering that the two 2D H-plane cuts for the Tx and Rx antennas collapse on a single 2D Tx/Rx plane. This is the approach used in ITER [4] and DEMO 2D simulations [5] and clearly is the most *extreme* of the 2D approximations to made. The computational cost of using a 3D code against a 2D code is confirmed by the wallclock timing of the runs. A 120, 000 iteration REFMUL3 run (using an hybrid MPI/OpenMP parallelisation) takes approximatly 7 hours on Marconi HPC Skylake partition, using 128 nodes with 4 MPI task/node and 12 OpenMP threads/task. To compare with the REFMUL (serial) run that takes 20 minutes on one core (a Marconi Skylake node can run several instances of the serial program at once, one per core). Figure 2—right displays a snapshot of the electric field E_z probing the slab plasma with a monostatic antenna setup taken at iteration $t_k = 100\times10^3$. Figure 3 shows 2D

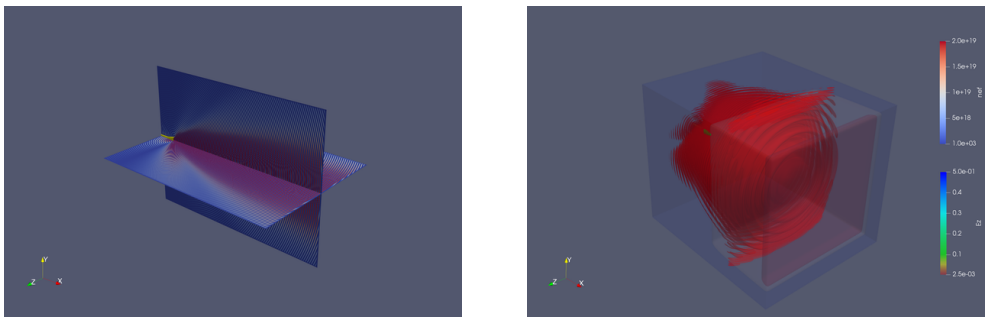

Figure 2. On the left, are presented the electric field E_z snapshot at iteration $t_k = 100 \times 10^3$ on the H-plane and E-planes of the horn antenna used. On the right, a snapshot of the electric field E_z probing the slab plasma with a monostatic antenna.

cuts of the 3D simulations taken at the H-plane of the antennas compared with the 2D simulations domains. For the MONO setup, A_1 displays the 3D (H-plane) and A_2 the 2D equivalence. In A_1, the *split* map is a representation artefact introduced to enhance the different amplitude evolutions in 3D and 2D. The lower half of the map uses contour levels that naturally fit the values of E_z in the H-plane. If the A_1 slice used the same contour levels used for the 2D case, in A_2, the result would be the one on the top half of the figure. It is clear that in 3D and 2D the decay in amplitude is radically different; B_1 displays the 3D (H-plane) of the transmission antenna and B_2 the 3D (H-plane) of the reception antenna for the BTOR setup. The 2D case does not exist for this case and is commonly approximated by A_2; for the BPOL antenna setup, the results for the 3D (H-plane) appear in C_1 while the 2D case is on C_2. One of the most important differences from 2D *against* 3D is the spatial evolution of the amplitude of E_z, seen qualitatively in the split contour values in A_1 (valid for the other cases as well). A quantitative look at this spacial evolution is offered in figure 4, where the values of E_z taken along the antennas' axes (LoS) for the different cases are shown. For the BTOR case the grey line repeats the 2D MONO case since it is closest approximation to the 3D case. The results confirms the different law of decay, $\propto R^{-1}$ for 3D and to $\propto (\log R\sqrt{R})^{-1}$ for 2D.

The main use of FMCW reflectometry is density profile measurement. The signal sent through the plasma propagates until being reflected at cutoff position. The phase shift suffered by the

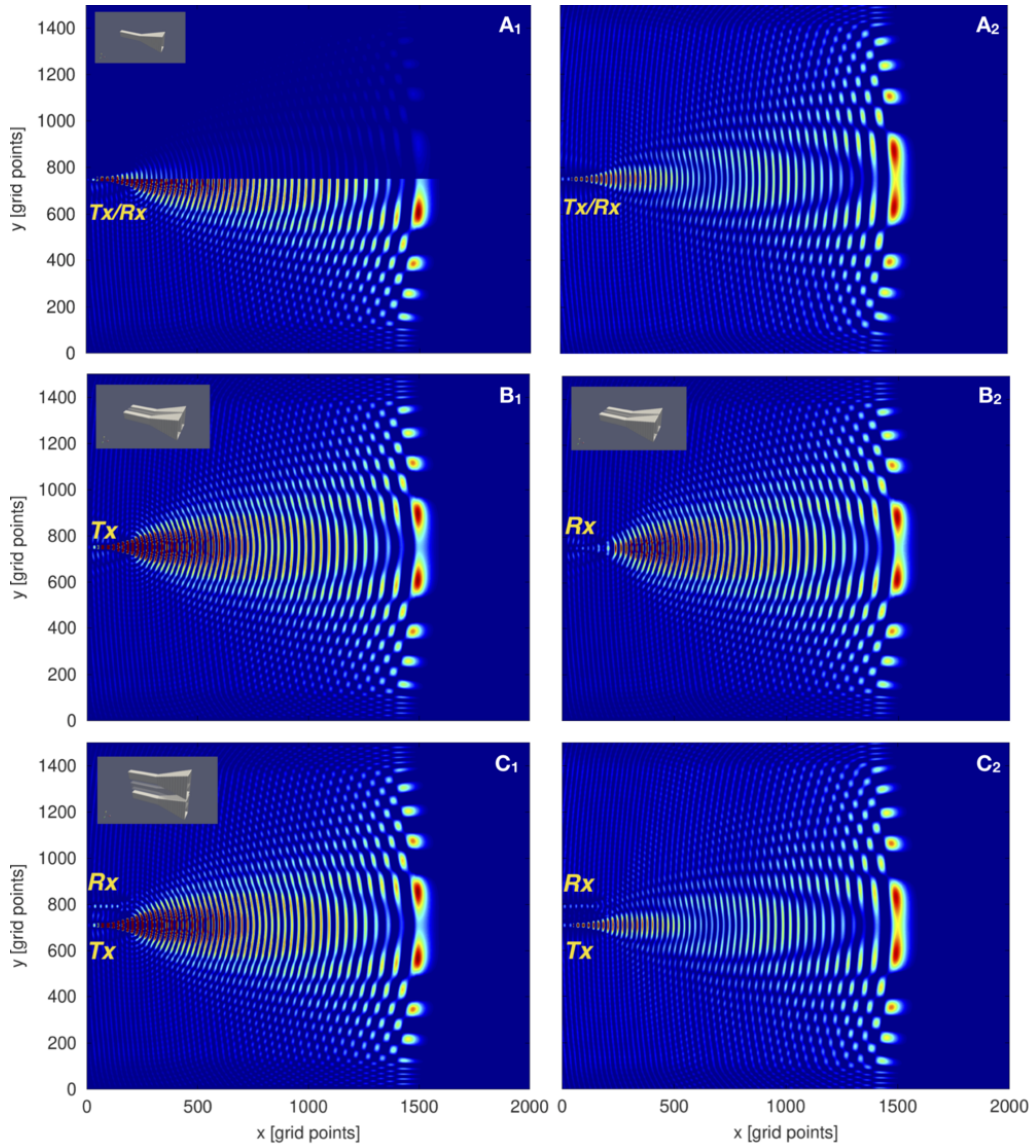

Figure 3. Electric field poloidal snapshots for the different antennas' arrangements used in 3D and 2D. The 3D field snapshots are plane cuts along the H-plane of the antennas and the 2D correspond to the entire simulated plane. A_1 3D (H-plane) of monostatic antenna and A_2 2D, monostatic antenna; B_1 3D (H-plane) of the transmission antenna for toroidally distributed bistatic setup and B_2 3D (H-plane) of the reception antenna for toroidally distributed bistatic setup; C_1 3D (H-plane) of the antennas for poloidally distributed bistatic setup and C_3 2D, poloidally distributed bistatic setup.

reflected wave φ_p reflects the propagation of the wave along a path described by a refraction index $N(R)$ and contains information on the electronic density n_e. Sweeping the probing frequency f an evolution of the phase with frequency can obtained $\partial\varphi/\partial f$ and through it the position of the density profile recovered. For a linear profile there is an analytic solution for $\partial\varphi/\partial f$

$$\frac{\partial\varphi}{\partial f} = \frac{4\pi^{3/2}\Gamma(1)(R_M - R0)}{c\Gamma(1.5)}\left(\frac{f}{f_M}\right)^2, \tag{4.1}$$

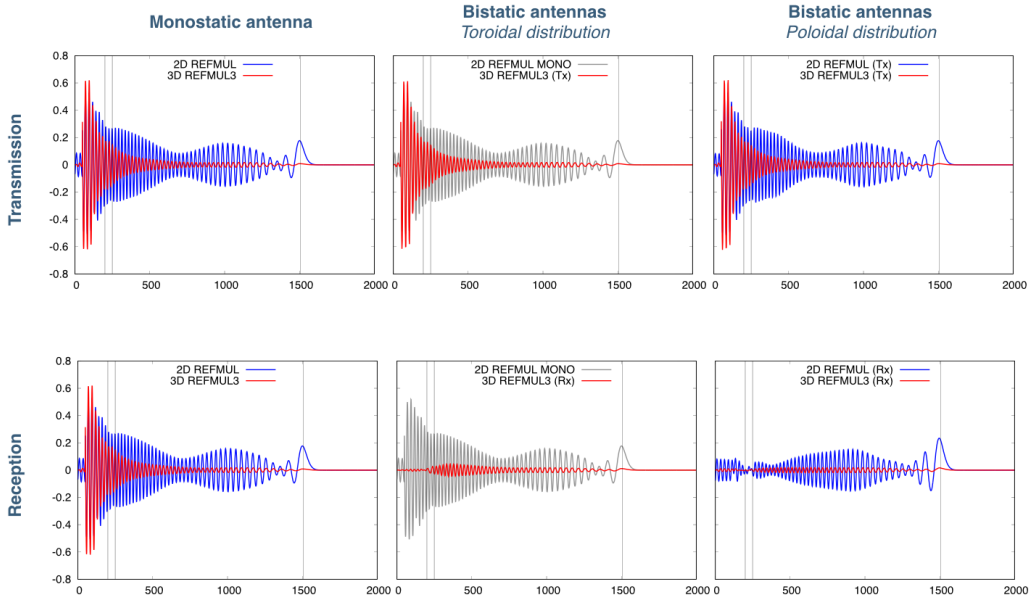

Figure 4. Electric field E_z sampled along the line of sight of the antennas (antennas' axes) for the different cases. The top row displays the cuts for the Tx antennas while the bottom row displays the cuts for the Rx antennas. Columnwise the results in the first column refer to the MONO case; the second to BTOR case (the grey line repeats the 2D MONO case, the closest approximation to the 3D BTOR case) and the third to the BPOL case. The first vertical line marks the antenna mouth; the second, the edge of the plasma; and the third, the cutoff position.

that can be compared with the simulated ones. Here R_M is the maximum reference position, corresponding to a frequency of f_M and $\Gamma(\cdot)$ is the Gamma function. Simulations results in 2D and 3D compare very favourable with theory for the MONO and BPOL cases while showing a slight deviation in the BTOR case but not enough to cause a major error in the positioning of the density profile. The BPOL case exhibits some amplitude modulation. In figure 5 we present the calculated error in position which falls within the 1 cm requirements for ITER PPR. The deviation in $\partial\varphi/\partial f$ in the BTOR case traduces in an augmented error for this case. The probable cause is the coupling

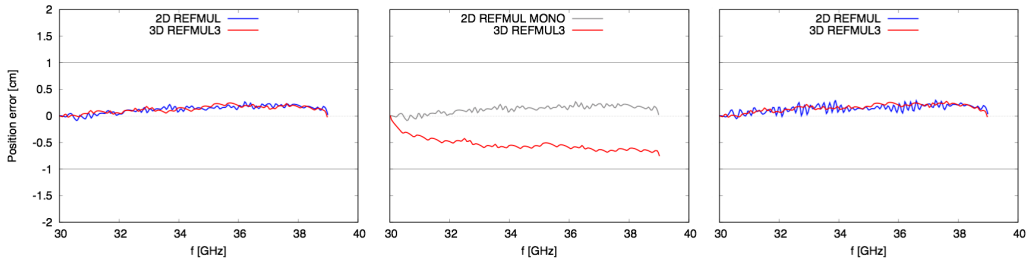

Figure 5. Comparison of the position error resulting from the 2D and 3D simulations for the three cases in study. On the left the MONO case, in the middle the BTOR (the grey line repeats the 2D MONO error, the closest approximation to the 3D BTOR case) and on the right the BPOL case. The horizontal grey lines mark the limits of the 1 cm error requirements for ITER PPR.

between the Tx and Rx antennas, made through the larger E-plane of the radiation diagram which has also a contributing secondary lobe.

5 Conclusions

This first study makes some important points not without consequence for reflectometry simulations. One has to do with the more realistic amplitude values given by 3D simulations. Assessing them is of major importance to have a proper signal-to-noise ratio (S/N), to infer the true impact of turbulence signatures in S/N or in the amelioration of profile initialisation. The phase is more robust than amplitudes in 2D simulations giving more confidence to 2D simulations in general and to ITER and DEMO in particular, which have dealt mainly with processing of $\partial\varphi/\partial f$. Results also point to the importance of the radiation diagram in the coupling of Tx and Rx antennas for the bistatic cases and its possible impact on 2D modelling of toroidal antennas' setup. Using the 2D approach in this case should be accompanied by a knowledge of the radiation pattern and when possible a 3D simulation to support or help to correct the model. Whenever a 2D model is enough, its use allows a much better use of computational resources as 3D simulations are, as seem before, computationally expensive and should be channelled to the cases where 2D is unable to provide an correct answer, as an aid to help setting up or calibrate a 2D case study or as a complement to the main 2D simulations.

Acknowledgments

This work has been carried out within the framework of the EUROfusion Consortium and has received funding from the Euratom research and training programme 2014-2018 and 2019-2020 under grant agreement No 633053 and within the framework of the French Federation for Magnetic Fusion Studies (FR-FCM). IST activities also received financial support from Fundação para a Ciência e Tecnologia through project UID/FIS/50010/2019. The views and opinions expressed herein do not necessarily reflect those of the European Commission.

References

[1] F. da Silva, M. C. Pinto, B. Després and S. Heuraux, *Stable explicit coupling of the yee scheme with a linear current model in fluctuating magnetized plasmas*, *J. Comput. Phys.* **295** (2015) 24.

[2] K. Yee, *Numerical solution of initial boundary value problems involving Maxwell's equations in isotropic media*, *IEEE Trans. Antennas Propagat.* **14** (1966) 302.

[3] C.A. Balanis, *Antenna Theory, Analysis and Design*, John Wiley and Sons (1982).

[4] F. da Silva, S. Heuraux, E. Ricardo, P. Quental and J. Ferreira, *Assessment of the measurement performance of the in-vessel systems of gaps 4 and 6 of the ITER Plasma Position Reflectometer using a FDTD Maxwell full-wave code*, presented at the *13th International Reflectometry Workshop for fusion plasma diagnostics*, Daejeon, South Korea, 10–12 May 2017.

[5] E. Ricardo, F. da Silva, S. Heuraux and A. Silva, *Assessment of the measurement performance of DEMO Plasma Position Reflectometry gaps perpendicular to the separatrix*, presented at the *12.° Congresso do Comité Português da URSI "Inteligência artificial e as ciências rádio"*, Lisbon, Portugal, 14 December 2018.